RESEARCH REPORT

STEM CELLS AND REGENERATION

Asymmetric inheritance of the apical domain and self-renewal of retinal ganglion cell progenitors depend on Anillin function

Alessio Paolini[1,*], Anne-Laure Duchemin[1,*], Shahad Albadri[1], Eva Patzel[1,2], Dorothee Bornhorst[1], Paula González Avalos[3], Steffen Lemke[3], Anja Machate[4], Michael Brand[4], Saadettin Sel[2], Vincenzo Di Donato[5], Filippo Del Bene[5], Flavio R. Zolessi[6], Mirana Ramialison[7] and Lucia Poggi[1,‡]

ABSTRACT

Divisions that generate one neuronal lineage-committed and one self-renewing cell maintain the balance of proliferation and differentiation for the generation of neuronal diversity. The asymmetric inheritance of apical domains and components of the cell division machinery has been implicated in this process, and might involve interactions with cell fate determinants in regulatory feedback loops of an as yet unknown nature. Here, we report the dynamics of Anillin – an essential F-actin regulator and furrow component – and its contribution to progenitor cell divisions in the developing zebrafish retina. We find that asymmetrically dividing retinal ganglion cell progenitors position the Anillin-rich midbody at the apical domain of the differentiating daughter. *anillin* hypomorphic conditions disrupt asymmetric apical domain inheritance and affect daughter cell fate. Consequently, the retinal cell type composition is profoundly affected, such that the ganglion cell layer is dramatically expanded. This study provides the first *in vivo* evidence for the requirement of Anillin during asymmetric neurogenic divisions. It also provides insights into a reciprocal regulation between Anillin and the ganglion cell fate determinant Ath5, suggesting a mechanism whereby the balance of proliferation and differentiation is accomplished during progenitor cell divisions *in vivo*.

KEY WORDS: Anillin, Asymmetric cell division, Ath5 (Atoh7), Neurogenesis, Retina development, Apical domain inheritance

INTRODUCTION

During retinal development, asymmetric self-renewing divisions of progenitor cells prolong the temporal progression of neurogenesis (Cayouette et al., 2006; Cepko, 2014; Parameswaran et al., 2014). The asymmetric inheritance of apical components has been suggested to provide instructive information for the specification of cell fate (Clark et al., 2012; Huttner and Brand, 1997; Kechad et al., 2012). The complex cellular and molecular interactions linking this inheritance to daughter cell self-renewal and differentiation *in vivo* remain elusive. Recent studies reported

[1]Department of Developmental Biology/Physiology, Centre for Organismal Studies (COS) Heidelberg, Im Neuenheimer Feld 230, Heidelberg 69120, Germany. [2]Department of Ophthalmology, University of Heidelberg, Heidelberg 69120, Germany. [3]Centre for Organismal Studies (COS) Heidelberg, Im Neuenheimer Feld 230, Heidelberg 69120, Germany. [4]Biotechnology Center and Center for Regenerative Therapies Dresden, TU Dresden, Fetscherstrasse 105, Dresden 01307, Germany. [5]Institut Curie - Centre de Recherche, U934/UMR3215, Paris 75248, Cedex 05, France. [6]Sección Biología Celular, Facultad de Ciencias, Universidad de la República and Institut Pasteur de Montevideo, 11400 Montevideo, Uruguay. [7]Australian Regenerative Medicine Institute, Monash University, Wellington Road, Clayton, Victoria 3187, Australia.
*These authors contributed equally to this work

‡Author for correspondence (lucia.poggi@cos.uni-heidelberg.de)

cleavage furrow components as potential signalling sources for instructing cell fate (Chen and Zhang, 2013; Dubreuil et al., 2007; Ettinger et al., 2011; Kosodo and Huttner, 2009; Pollarolo et al., 2011; Singh and Pohl, 2014). For example, newborn sensory neurons of the *Drosophila* notum inherit asymmetrically distributed cytokinesis remnants of the last mitotic cleavage (Pollarolo et al., 2011). Other studies have suggested that the extent of release of the post-mitotic midbody – a transient intercellular bridge from the cleavage furrow just before abscission – couples cell division to cell fate in neuroepithelial, stem and cancer cells (Dubreuil et al., 2007; Ettinger et al., 2011). It remains unknown whether cleavage furrow components also instruct asymmetric cell division *in vivo* in the developing vertebrate neuroepithelium.

Here, we combined *in vivo* time-lapse confocal imaging with cell biology and functional analyses to examine the role of the F-actin-binding protein Anillin – a crucial component of the cleavage furrow and midbody (Field and Alberts, 1995; Kechad et al., 2012; Rincon and Paoletti, 2012; Ronkainen et al., 2011) – in the occurence of asymmetric divisions in the developing zebrafish retina. We report novel evidence supporting that Anillin is important not only for progenitor cell self-renewal, but also for balancing symmetric and asymmetric outcomes essential for correct retinal neurogenesis. This study further provides novel insights into the interplay between cytokinesis machinery components and the retinal ganglion cell (RGC) fate determinant Ath5 (Atoh7) during asymmetric neurogenic cell divisions *in vivo*.

RESULTS AND DISCUSSION

Dynamic expression of Anillin suggests a role in asymmetric divisions generating RGCs
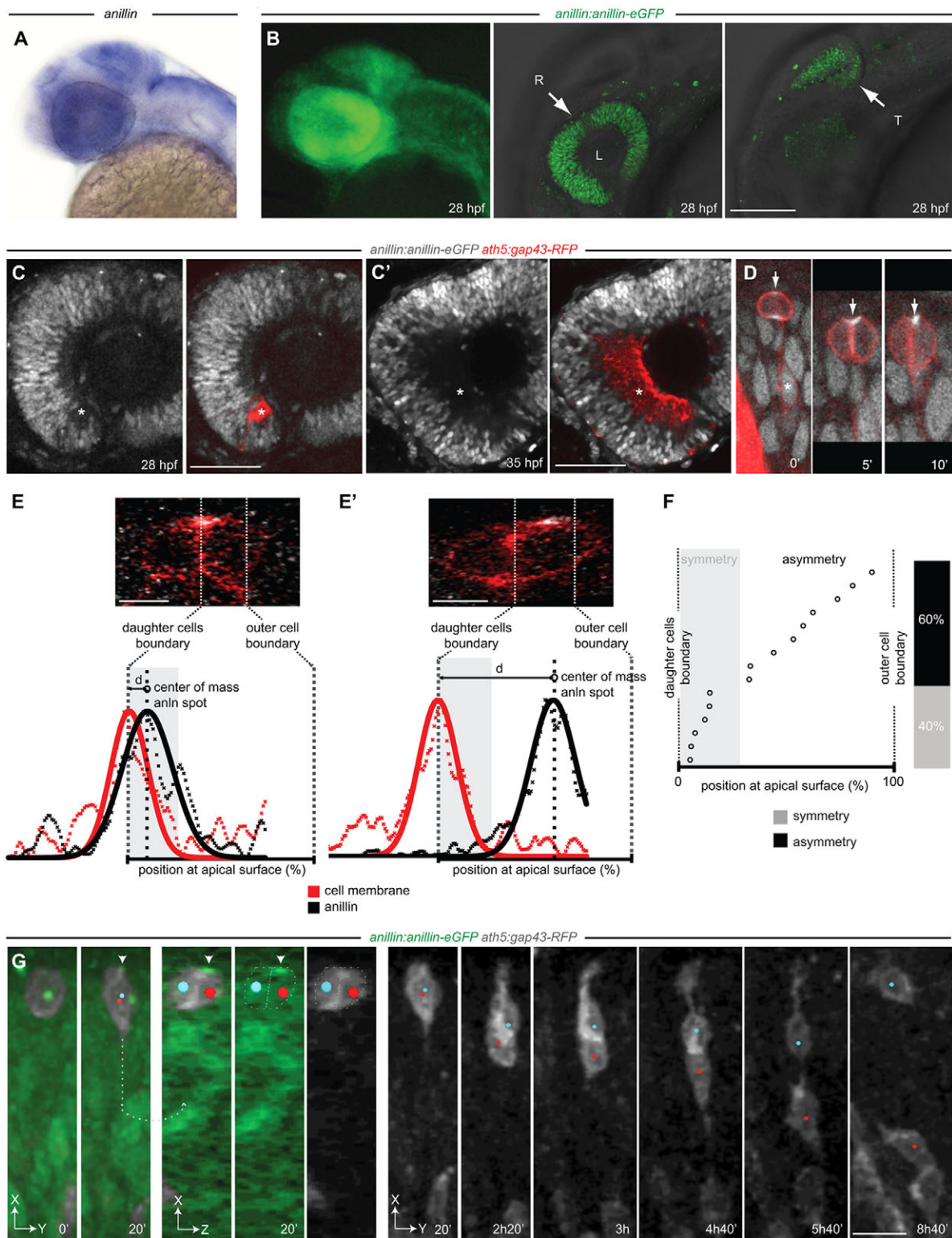
To investigate the role of Anillin during retinal neurogenesis we established an *anillin:anillin-eGFP* transgenic line that recapitulates *anillin* expression *in vivo* (Fig. 1A,B). All cells in the retinal neuroepithelium are proliferative prior to 28 hours post fertilisation (hpf) (Li et al., 2000), strongly expressing *anillin* (Fig. 1B). The *ath5: gap43-RFP* transgene, in which membrane-tethered RFP (Gap43-RFP) is expressed under the control of the *ath5* promoter (Zolessi et al., 2006), highlights the cell cycle exit of RGCs – the first-born neurons in the vertebrate retina. Time-lapse imaging in double-transgenic *anillin:anillin-eGFP;ath5:gap43-RFP* embryos revealed that *anillin:anillin-eGFP* is downregulated in the differentiating Gap43-RFP-positive cells of the RGC layer, suggesting *anillin* downregulation by Ath5 (Fig. 1C,C′). Consistently, retinae from *lakritz* mutant (*ath5*$^{-/-}$) embryos, in which progenitors undergo extra rounds of proliferative divisions instead of differentiating into RGCs (Jusuf et al., 2012; Kay et al., 2001; Kelsh et al., 1996), failed to downregulate *anillin* mRNA (supplementary material Fig. S1A). The presence of a well-characterised Ath5 consensus binding site

DEVELOPMENT

Fig. 1. Anillin expression during zebrafish retinal differentiation. (A) *anillin* mRNA (blue) at 28 hpf. (B) Expression of the *anillin-eGFP* transgene. R, retina; T, optic tectum; L, lens. Left, *z*-projection view; middle and right, *z*-plane. (C,C′) *anillin:anillin-eGFP/ath5:gap43-RFP* transgenic retina. *anillin*-eGFP is downregulated in the differentiating cells of the RGC layer (asterisks). (D) Anillin-GFP localisation in the nucleus (asterisk), cleavage furrow (arrow, *t*=0′) and at the midbody (arrow, *t*=5′ and *t*=10′). Time, minutes. (E,E′) Anillin-eGFP symmetric (E) and asymmetric (E′) distribution and intensity profiles (data points and fitted Gaussian) used to detect the offset of the Anillin-eGFP spot from the daughter cell boundary. (F) The position of apical Anillin-eGFP (*n*=15 divisions). Distance from the cell boundary within the average radius of the Anillin spot (grey) is used to define symmetry (see supplementary material Fig. S3). (G) Frames from supplementary material Movie 1. The Anillin-eGFP spot-inheriting daughter (white arrowhead, red dot) migrates to the RGC layer. The sibling (blue dot) migrates back to the apical surface (*n*=5 out of 5 analysed divisions). At *t*=20′ a rotated frontal *z*-section (dotted lines, 3D slicing mode) across the centre of the dividing daughters is shown (oriented along the *z*-plane). The apical surface of the retinal neuroepithelium is to the top. Scale bars: 110 μm in B; 25 μm in C,C′; 6 μm in E,E′; 12 μm in G.

(CACCTG) (Del Bene et al., 2007) in an active enhancer region upstream of *anillin* [highlighted by histone H3 lysine 4 mono-methylation (H3K4me1) mark] (supplementary material Fig. S1B) further suggests that Ath5 directly regulates *anillin*.

Anillin is an established midbody component, and asymmetric inheritance of the midbody during stem cell division has been reported in multiple systems, including mouse radial glial progenitors (Dubreuil et al., 2007; Ettinger et al., 2011; Hesse et al., 2012; Kosodo et al., 2004). This led us to investigate Anillin-eGFP dynamics in dividing retinal progenitor cells. Live imaging confirmed the localisation of Anillin-eGFP in the *gap43-RFP*-expressing progenitor cell nuclei at interphase (asterisk, Fig. 1D, t=0′), to the contractile ring during cytokinesis (arrow, Fig. 1D, t=0′) and at the daughter cell apical interface consistent with the formation of a midbody at the end of cytokinesis (Fig. 1D, t=5′ and t=10′). Interestingly, 60% of analysed divisions (n=9 out of 15) displayed asymmetric positioning of the Anillin-eGFP spot to one daughter cell apical domain at the end of cytokinesis (Fig. 1E-F). Consistent with a correlation between Anillin-eGFP inheritance and cell fate, we observed that the daughter cell inheriting the Anillin-eGFP spot retracts its apical process and migrates basally towards the differentiating RGC layer, while the sibling cell invariably migrates back towards the apical surface (n=5 out of 5, Fig. 1G; supplementary material Movie 1). In addition to the observed dynamics of *anillin* expression downstream of Ath5, these data are consistent with a role for Anillin in asymmetric neurogenic cell divisions *in vivo*.

Apical domain distribution depends on Anillin
To test the role of Anillin in retinal neurogenesis we performed a loss-of-function analysis. Anillin knockdown causes cytokinesis defects that affect early vertebrate development (Gbadegesin et al., 2014; Reyes et al., 2014) (supplementary material Movie 2). We therefore generated *anillin* hypomorphic conditions (supplementary material Fig. S2A-C) and performed all analyses in mosaic zebrafish embryos as previously described (Jusuf et al., 2012). Live imaging of dividing transplanted progenitor cells labelled with H2B-RFP (nuclei, red) and LifeAct-Venus (F-actin, yellow; Riedl et al., 2008) highlighted the appearance of an F-actin-enriched spot at the basal side of the cell body before anaphase (Kosodo et al., 2008) and its basal-apical displacement during cytokinesis (supplementary material Fig. S2D,E), indicating that vertical furrowing progresses normally in the mononucleated *anillin* hypomorphic cells.

The midbody has been reported as a positional cue for apical F-actin accumulation at the daughter cell interface before the formation of new cell-cell junctions (Herszterg et al., 2013; Morais-de-Sa and Sunkel, 2013; Singh and Pohl, 2014). Expression of the *anillin-eGFP* reporter together with a red *lifeact-Ruby* construct revealed that midbody formation at the end of cytokinesis indeed coincides with the transient accumulation of F-actin around it (arrow, Fig. 2A; supplementary material Movie 3). Consistent with the apical Anillin-eGFP spot, quantification of LifeAct-Venus intensity revealed that more than half of the analysed divisions (57%, n=8 out of 14) distribute the apical F-actin-rich domain asymmetrically to one daughter (Fig. 2B,C; supplementary material Movie 4). This asymmetric distribution is drastically reduced in *anillin* hypomorphic conditions (15%, n=2 out of 13) (Fig. 2B,C; supplementary material Movie 5), indicating that Anillin is

required for proper apical domain segregation in dividing retinal progenitor cells.

The evolutionarily conserved apical polarity protein Par3 (Pard3) colocalises with Factin at the level of junctional belts in neuroepithelial cells and its inheritance during cell division has been linked to neuronal fate (Alexandre et al., 2010; Bultje et al., 2009; Chen and Zhang, 2013; Dong et al., 2012; Shi et al., 2003; Takekuni, 2003; Zolessi et al., 2006). We investigated whether Par3 asymmetric inheritance depends on Anillin. Time-lapse imaging of a Par3-GFP protein revealed that, whereas in control clones most divisions distribute Par3 asymmetrically (80%, n=12 out of 15, Fig. 2D; supplementary material Movie 6), *anillin* hypomorphic conditions favour symmetric Par3 distribution (Fig. 2D, n=15 out of 15; supplementary material Movie 7). Thus, Anillin is required for the correct apical distribution of F-actin and Par3, which might be essential for asymmetric cell fate outcome.

anillin hypomorphic conditions affect retinal neurogenesis and the balance of symmetric and asymmetric RGC progenitor divisions
We next assessed whether the observed effect on Par3 and F-actin reflects changes in the mode of cell division. Hypomorphic *anillin* conditions produce an overall increase in *ath5:GFP* (Poggi et al., 2005) or *ath5:gap43-RFP* transgene expression (Fig. 3A-C; supplementary material Movies 8 and 9) and an expansion of the RGC layer (Fig. 3C), which is efficiently rescued by co-injection of *anillin-eGFP* mRNA (Fig. 3D). Although quantification of phospho-histone H3 (pH3)-positive cells at 30 hpf revealed no significant difference between the control and *anillin* hypomorphic conditions (Fig. 3E,F), the number of pH3-positive cells within the *ath5:GFP* population was significantly lower in *anillin* hypomorphic conditions (Fig. 3E,G). Thus, retinal progenitor divisions are more likely to generate *ath5*-expressing daughters, and *ath5*-expressing cells are less likely to undergo further rounds of cell division.

To assess this hypothesis we performed *in vivo* time-lapse analysis of daughter cell fate in clones transplanted from *ath5:GFP* transgenic embryos. We considered symmetric versus asymmetric divisions based on two criteria: (1) Ath5:GFP positive (A) versus Ath5:GFP negative (self-renewing progenitor, P) in sibling daughters from divisions of H2B-RFP-labelled cells; (2) neuronal fate (N) versus self-renewing progenitor (P) in sibling daughters from divisions of H2B-RFP/Ath5:GFP-positive cells (Fig. 4) (Poggi et al., 2005). We found that 56% of divisions of H2B-RFP-positive cells were asymmetric, generating one GFP-positive and one GFP-negative daughter (A/P) (n=5 out of 9) (Fig. 4A,D; supplementary material Movie 10). By contrast, all divisions analysed in *anillin* hypomorphic clones were symmetric, entailing GFP in both daughter cells (Fig. 4B-D; supplementary material Movie 11) (n=10). This is consistent with the observed increase in Ath5:GFP-positive cells. Within the Ath5:GFP-positive control clones most analysed divisions (82%, n=9 out of 11) were asymmetric, generating one post-mitotic daughter, which retracts the apical process and migrates to the RGC layer, and one self-renewing progenitor (N/P) (Fig. 4A,D; supplementary material Movie 12) (Jusuf et al., 2012). The concomitant appearance of an extending axon from the cell body or expression of the *cxcr4b:cxcr4b-GFP* transgene (Donà et al., 2013) further indicated differentiation into an RGC (data not shown; Fig. 4C,C′) (Pujic et al., 2006). Conversely, most divisions in *anillin* hypomorphic clones were symmetric, generating two Cxcr4b-GFP-positive daughters (N/N; 70%, n=7 out
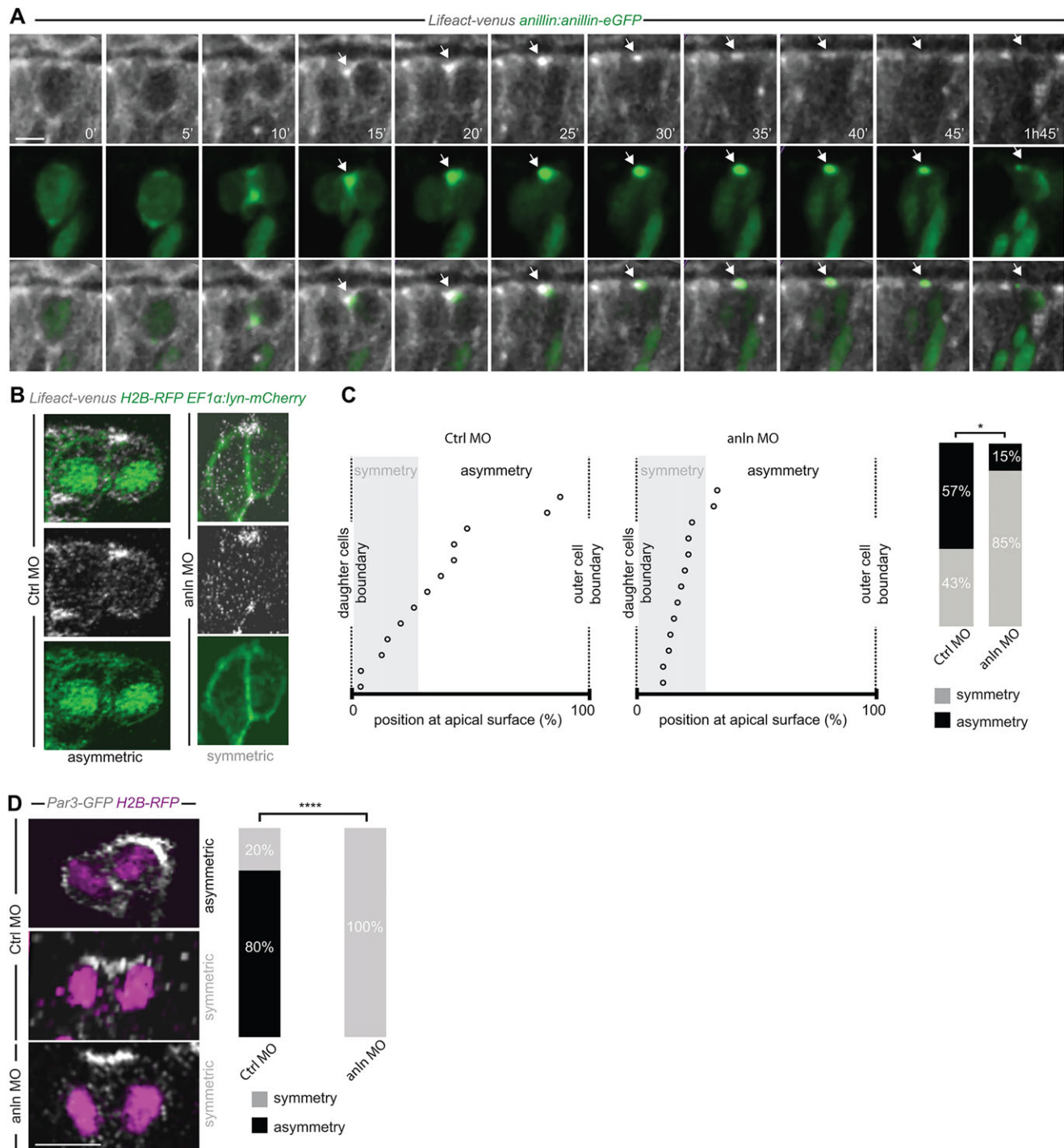
Fig. 2. Anillin is required for the apical distribution of F-actin and Par3. (A) Frames from supplementary material Movie 3. F-actin accumulates at the Anillin-eGFP-labelled midbody (arrow) at the end of cytokinesis. (B) Asymmetric (CtrlMO; frames from supplementary material Movie 4) and symmetric (anlnMO; frame from supplementary material Movie 5) distribution of apical F-actin accumulation. (C) Position of the apical F-actin-rich domain (CtrlMO, $n=14$; anlnMO, $n=13$) (as described in Fig. 1E-F and supplementary material Fig. S3); the frequency of asymmetry is 57% in CtrlMO and 15% in anlnMO (Wilcoxon Mann–Whitney test, $*P<0.05$). (D) Symmetric versus asymmetric inheritance of Par3 in CtrlMO (frame from supplementary material Movie 6) and anlnMO (frame from supplementary material Movie 7) injected embryos (two-tailed Fisher's exact test, $****P=10^{-4}$, CtrlMO, $n=15$; anlnMO, $n=15$). All images represent a single z-plane of a confocal stack. The apical surface of the retinal neuroepithelium is to the top. Scale bars: 4.8 μm in A; 5 μm in D.

of 10) (Fig. 4B-D; supplementary material Movie 13). This is consistent with the decrease in pH3-positive cells among the Ath5: GFP population. Hence, when Anillin function is impaired, retinal progenitors undergo symmetric rather than asymmetric divisions, in which they are more likely to upregulate *ath5*, become post-mitotic and adopt a neuronal (RGC) fate (Fig. 4E).

Conclusions

Our study provides compelling evidence that Anillin contributes to the regulation of asymmetric neurogenic cell divisions in the retinal neuroepithelium – favouring the maintenance of proliferating progenitors while also being required for the proper distribution of F-actin and Par3 at the daughter cell
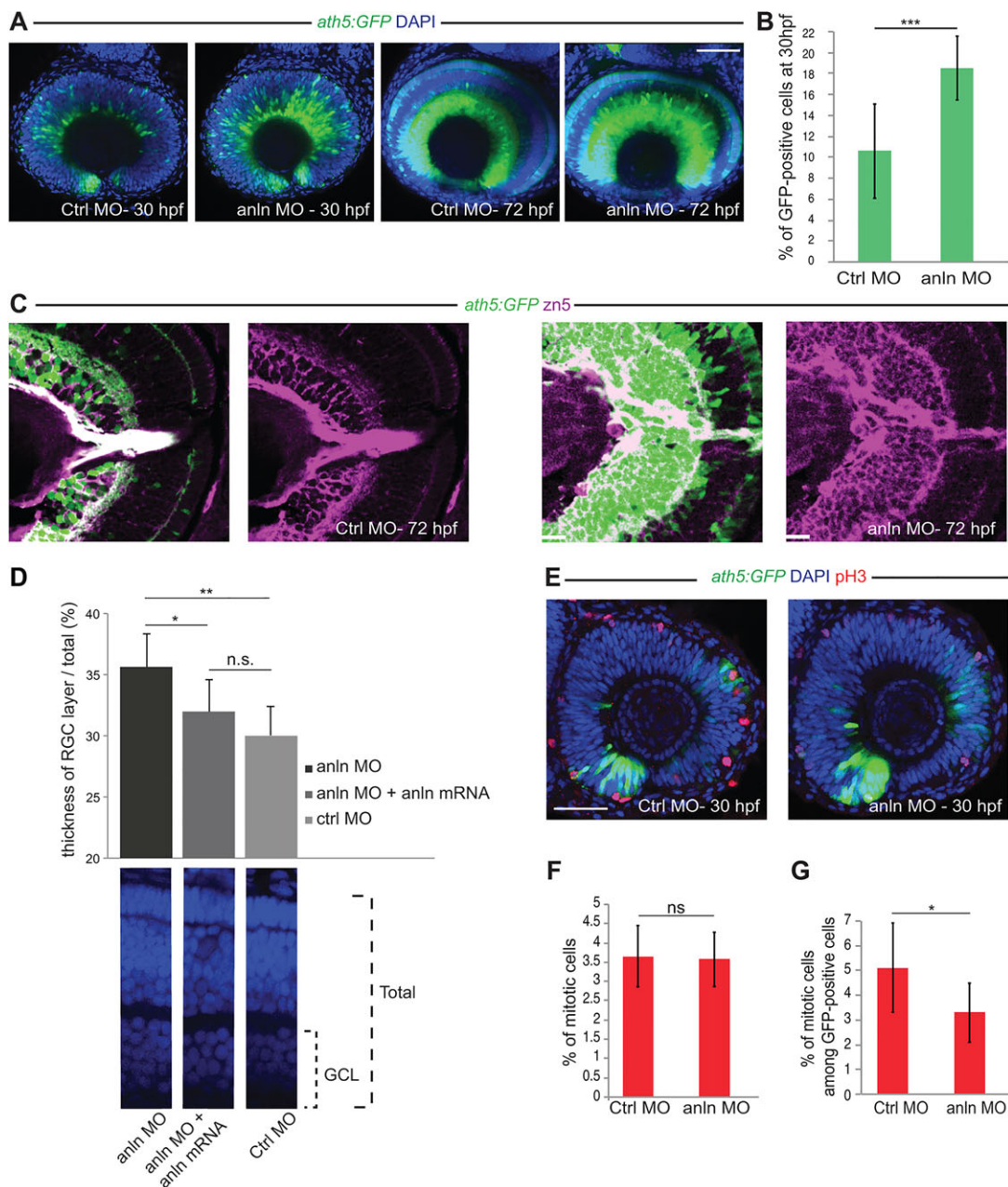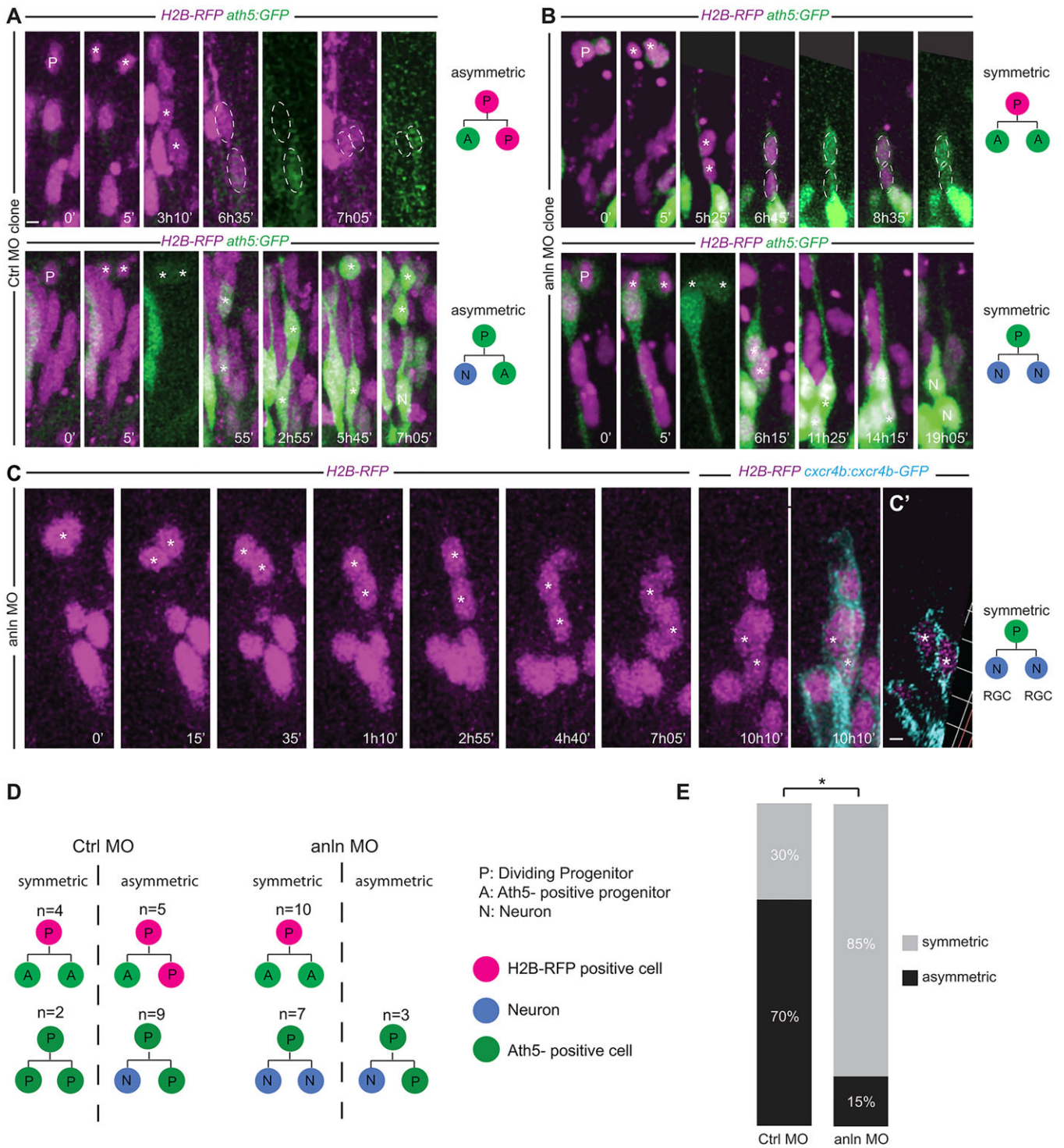
Fig. 3. *anillin* hypomorphic conditions affect RGC number. (A) anlnMO-injected retinae (*z*-projections) showing increase of Ath5:GFP signal (CtrlMO, *n*=24; anlnMO, *n*=31). (B) Quantification of GFP-positive among total (DAPI) cells, which increased from 10.5±1.6% (s.e.m.) in CtrlMO to 18.5±1.2% (s.e.m.) in anlnMO (Student's *t*-test, ***P<0.001; CtrlMO, *n*=8; anlnMO, *n*=7). (C) Retina frontal sections. Zn5 (Alcama) staining reveals expansion of the RGC layer in anlnMO retinae. (D) Rescue of the anlnMO phenotype. Student's *t*-test, *P<0.05, **P<0.01; n.s., not significant (*P*=0.11); anlnMO and CtrlMO, *n*=7; anlnMO+anln-eGFP mRNA, *n*=8. GCL, ganglion cell layer. (E) Phospho-histone H3 (pH3) labelling of mitotic cells (*z*-projections). (F) Ratio of pH3-positive among total DAPI-positive cells; 3.65±0.3% CtrlMO, 3.57±0.3% anlnMO (Student's *t*-test, *P*=0.46; CtrlMO, *n*=8; anlnMO, *n*=7). (G) Ratio of pH3-positive cells among GFP-positive cells is 5.1±0.6% for CtrlMO versus 3.3±0.5% for anlnMO (Student's *t*-test, *P<0.05; CtrlMO, *n*=8; anlnMO, *n*=7). Scale bars: 42 µm in A,E; 23.5 µm in C.

apical domain. Our time-lapse analysis of asymmetric cell divisions of RGC progenitors suggests that the differentiating (RGC) daughter transiently inherits the Anillin-eGFP-labelled midbody. This is in agreement with the idea that instructive information accompanying this inheritance is linked to neural fate commitment (Alexandre et al., 2010; Pollarolo et al., 2011; Zolessi et al., 2006).

This study establishes a framework for future mechanistic investigations to address how apical Anillin, F-actin and associated signalling molecules contribute to long-term fate decisions in asymmetric neurogenic cell divisions (Galvagni et al., 2012; Parameswaran et al., 2014). The nature of this information (e.g. cell cycle exit, cell polarity or neuronal fate acquisition) and the underlying signalling pathways have yet to be determined, but the evidence provided here suggests that they are likely to integrate feedback regulatory loops between *ath5* and *anillin*. Anillin expression correlates with the proliferation and metastatic potential of human tumours from many different tissue origins (Hall et al., 2005). Therefore, it is tempting to speculate that similar

Fig. 4. *anillin* hypomorphic conditions affect the balance between symmetric and asymmetric cell division of RGC progenitors. (A,B) Frames from supplementary material Movies 10-13 showing examples of symmetric and asymmetric division outcomes in the CtrlMO (A) and anlnMO (B) conditions. GFP intensity differences for A/P and A/A divisions were quantified ($P<0.05$ for CtrlMO clones; $P=0.92$ for anlnMO clones). (C) Division (asterisk) generating two Cxcr4b-eGFP-positive daughters (cyan) (10 h 10′). Each time frame represents a *z*-projection. (C′) A single *z*-stack. (D,E) Symmetric divisions increase from 30% in the CtrlMO to 85% in the anlnMO (two-tailed Fisher's exact test, *$P=0.011$). Apical surface of the retinal neuroepithelium is to the top. Scale bars: 5 µm in A,B; 5.5 µm in C,C′.

mechanisms, whereby components of the cytokinesis machinery contribute to maintaining the intrinsic asymmetry of proliferative divisions, might be common to all proliferating stem and progenitor cells.

MATERIALS AND METHODS
Animals

welfare agencies and in accordance with local (Tierschutzgesetz 111 Abs. 1 Nr. 1) and European Union animal welfare guidelines. For imaging, embryos were treated with 0.0045% 1-phenyl-2-thiourea (Sigma) to delay pigment formation. Lines used are indicated in the supplementary Materials and Methods.

Morpholinos

Morpholinos (1 ng/µl) were: CtrlMO, 5′-CCTCTTACCTCAGTTACAAT-TTATA-3′ (Gene Tools); ATGMO, 5′-GTACGCTACAAGCTGAAAG-TAAAGT-3′; and SpMO, 5′-TTTCACAAAAAGCTCTCACCTCGGT-3′. Controls and rescue experiments are described in the supplementary Materials and Methods.

pH3/Ath5:GFP analysis

The Cell Counter plugin from Fiji software was used to determine the average ratio of pH3-positive cells among total cells (DAPI staining) or among Ath5:GFP cells in every 2 µm of a 16 µm-thick *z*-projection.

Plasmids

Six plasmids were used: *BAC/anillin:anillin-eGFP* and *CMV:anln-eGFP_pDestTol2* (see supplementary Materials and Methods for cloning details and BAC transgenesis); *pCS2+:H2B-RFP* (Jusuf et al., 2012); *pCS2+:Lifeact-Venus* (kindly provided by R. Köster, TU Braunschweig, Germany); *pDestTol2/CMVSP6:lifeact-Ruby* vector (generated by I. Weisswange and kindly provided by J. Wittbrodt, University of Heidelberg, Germany); and *pCS2+:pard3-GFP* (kindly provided by P. Alexandre and J. Clarke, King's College London, UK).

Immunofluorescence and *in situ* hybridisation (ISH)

Immunostaining was performed as described (Jusuf et al., 2012; supplementary Materials and Methods). Primary antibodies: rabbit anti-phospho-histone H3 (Millipore, 06-570; 1:500), mouse anti-Zn5 (ZIRC Zn-5; 1:200) and chicken anti-GFP (Life Technologies, A10262; 1:200). Secondary antibodies: goat anti-rabbit IgG (H+L) conjugated to Cy5 (Invitrogen, A10523; 1:500), goat anti-mouse IgG (H+L) conjugated to Alexa fluor 546 (Invitrogen, A11003; 1:500) and donkey anti-chicken IgG (H+L) conjugated to Alexa fluor 488 (Jackson, 703-546-155; 1:250). Nuclei were counterstained with DAPI (Sigma; 1:1000).

For ISH, antisense probes for *anillin* and *ath5* were generated as previously described (Schuhmacher et al., 2011). See supplementary Materials and Methods for cloning and ISH protocol details.

Imaging

A Leica SpE confocal laser scanning microscope was used with a Leica 40×1.15 NA oil-immersion or Leica 63×1.2 NA water-immersion objective and Leica Application Suite (LAS) software (see supplementary Materials and Methods for further details of imaging). Volocity software (version 5.3, PerkinElmer) or Fiji was used for image processing and analyses. For analysis of F-actin spot displacement (supplementary material Fig. S2), coordinates (x, y, z) of the spot at the basal side of the cell body at anaphase and at the apical surface at telophase were determined. Distance covered and velocity were calculated between the two points. For lineage analysis, mosaic clones were randomly selected in the time-lapse series and daughter cells tracked manually in 4D after division. For A/P and A/A divisions (Fig. 4A,B), the ratio GFP intensity/background was assessed with Fiji. Analysis of Anillin and F-actin distributions is described in supplementary material Fig. S3 legend. Par3-GFP distribution was assessed on frontal *z*-sections across the centre of the dividing daughters (Alexandre et al., 2010).

Statistical analysis

Statistical tests were performed using Prism 5.0 (GraphPad), Microsoft Excel and R (Fisher's exact test, Student's *t*-test and Wilcoxon Mann–Whitney test) with $P<0.05$ considered significant. Classification of the distance between the daughter cell interface and Anillin/F-actin centre of mass was performed using R. For comparison between CtrlMO and anlnMO we used unpaired homoscedastic two-tailed Student's *t*-test

[lineage analysis (GFP-positive daughters), rescue of the RGC layer, F-actin spot displacement], Wilcoxon Mann–Whitney test (F-actin distribution in CtrlMO versus anlnMO conditions) and two-tailed Fisher's exact test (Par3 inheritance and lineage studies). All data represent three or more independent experiments.

Supplementary material

Supplementary material available online at
http://dev.biologists.org/lookup/suppl/doi:10.1242/dev.118612/-/DC1

References

Alexandre, P., Reugels, A. M., Barker, D., Blanc, E. and Clarke, J. D. W. (2010). Neurons derive from the more apical daughter in asymmetric divisions in the zebrafish neural tube. *Nat. Neurosci.* **13**, 673-679.

Bultje, R. S., Castaneda-Castellanos, D. R., Jan, L. Y., Jan, Y.-N., Kriegstein, A. R. and Shi, S.-H. (2009). Mammalian Par3 regulates progenitor cell asymmetric division via notch signaling in the developing neocortex. *Neuron* **63**, 189-202.

Cayouette, M., Poggi, L. and Harris, W. A. (2006). Lineage in the vertebrate retina. *Trends Neurosci.* **29**, 563-570.

Cepko, C. (2014). Intrinsically different retinal progenitor cells produce specific types of progeny. *Nat. Rev. Neurosci.* **15**, 615-627.

Chen, J. and Zhang, M. (2013). The Par3/Par6/aPKC complex and epithelial cell polarity. *Exp. Cell Res.* **319**, 1357-1364.

Clark, B. S., Cui, S., Miesfeld, J. B., Klezovitch, O., Vasioukhin, V. and Link, B. A. (2012). Loss of Llgl1 in retinal neuroepithelia reveals links between apical domain size, Notch activity and neurogenesis. *Development* **139**, 1599-1610.

Del Bene, F., Ettwiller, L., Skowronska-Krawczyk, D., Baier, H., Matter, J.-M., Birney, E. and Wittbrodt, J. (2007). In vivo validation of a computationally predicted conserved Ath5 target gene set. *PLoS Genet.* **3**, e159.

Donà, E., Barry, J. D., Valentin, G., Quirin, C., Khmelinskii, A., Kunze, A., Durdu, S., Newton, L. R., Fernandez-Minan, A., Huber, W. et al. (2013). Directional tissue migration through a self-generated chemokine gradient. *Nature* **503**, 285-289.

Dong, Z., Yang, N., Yeo, S.-Y., Chitnis, A. and Guo, S. (2012). Intralineage directional notch signaling regulates self-renewal and differentiation of asymmetrically dividing radial glia. *Neuron* **74**, 65-78.

Dubreuil, V., Marzesco, A.-M., Corbeil, D., Huttner, W. B. and Wilsch-Bräuninger, M. (2007). Midbody and primary cilium of neural progenitors release extracellular membrane particles enriched in the stem cell marker prominin-1. *J. Cell Biol.* **176**, 483-495.

Ettinger, A. W., Wilsch-Bräuninger, M., Marzesco, A.-M., Bickle, M., Lohmann, A., Maliga, Z., Karbanová, J., Corbeil, D., Hyman, A. A. and Huttner, W. B. (2011). Proliferating versus differentiating stem and cancer cells exhibit distinct midbody-release behaviour. *Nat. Commun.* **2**, 503.

Field, C. M. and Alberts, B. M. (1995). Anillin, a contractile ring protein that cycles from the nucleus to the cell cortex. *J. Cell Biol.* **131**, 165-178.

DEVELOPMENT

Galvagni, F., Baldari, C. T., Oliviero, S. and Orlandini, M. (2012). An apical actin-rich domain drives the establishment of cell polarity during cell adhesion. *Histochem. Cell Biol.* **138**, 419-433.

Gbadegesin, R. A., Hall, G., Adeyemo, A., Hanke, N., Tossidou, I., Burchette, J., Wu, G., Homstad, A., Sparks, M. A., Gomez, J. et al. (2014). Mutations in the gene that encodes the F-actin binding protein anillin cause FSGS. *J. Am. Soc. Nephrol.* **25**, 1991-2002.

Hall, P. A., Todd, C. B., Hyland, P. L., McDade, S. S., Grabsch, H., Dattani, M., Hillan, K. J. and Russell, S. E. H. (2005). The septin-binding protein anillin is overexpressed in diverse human tumors. *Clin. Cancer Res.* **11**, 6780-6786.

Herszterg, S., Leibfried, A., Bosveld, F., Martin, C. and Bellaïche, Y. (2013). Interplay between the dividing cell and its neighbors regulates adherens junction formation during cytokinesis in epithelial tissue. *Dev. Cell* **24**, 256-270.

Hesse, M., Raulf, A., Pilz, G.-A., Haberlandt, C., Klein, A. M., Jabs, R., Zaehres, H., Fügemann, C. J., Zimmermann, K., Trebicka, J. et al. (2012). Direct visualization of cell division using high-resolution imaging of M-phase of the cell cycle. *Nat. Commun.* **3**, 1076.

Huttner, W. B. and Brand, M. (1997). Asymmetric division and polarity of neuroepithelial cells. *Curr. Opin. Neurobiol.* **7**, 29-39.

Jusuf, P. R., Albadri, S., Paolini, A., Currie, P. D., Argenton, F., Higashijima, S.-I., Harris, W. A. and Poggi, L. (2012). Biasing amacrine subtypes in the Atoh7 lineage through expression of Barhl2. *J. Neurosci.* **32**, 13929-13944.

Kay, J. N., Finger-Baier, K. C., Roeser, T., Staub, W. and Baier, H. (2001). Retinal ganglion cell genesis requires lakritz, a zebrafish atonal Homolog. *Neuron* **30**, 725-736.

Kechad, A., Jananji, S., Ruella, Y. and Hickson, G. R. X. (2012). Anillin acts as a bifunctional linker coordinating midbody ring biogenesis during cytokinesis. *Curr. Biol.* **22**, 197-203.

Kelsh, R. N., Brand, M., Jiang, Y. J., Heisenberg, C. P., Lin, S., Haffter, P., Odenthal, J., Mullins, M. C., van Eeden, F. J., Furutani-Seiki, M. et al. (1996). Zebrafish pigmentation mutations and the processes of neural crest development. *Development* **123**, 369-389.

Kimmel, C. B., Ballard, W. W., Kimmel, S. R., Ullmann, B. and Schilling, T. F. (1995). Stages of embryonic development of the zebrafish. *Dev. Dyn.* **203**, 253-310.

Kosodo, Y. and Huttner, W. B. (2009). Basal process and cell divisions of neural progenitors in the developing brain. *Dev. Growth Differ.* **51**, 251-261.

Kosodo, Y., Röper, K., Haubensak, W., Marzesco, A.-M., Corbeil, D. and Huttner, W. B. (2004). Asymmetric distribution of the apical plasma membrane during neurogenic divisions of mammalian neuroepithelial cells. *EMBO J.* **23**, 2314-2324.

Kosodo, Y., Toida, K., Dubreuil, V., Alexandre, P., Schenk, J., Kiyokage, E., Attardo, A., Mora-Bermúdez, F., Arii, T., Clarke, J. D. W. et al. (2008). Cytokinesis of neuroepithelial cells can divide their basal process before anaphase. *EMBO J.* **27**, 3151-3163.

Li, Z., Hu, M., Ochocinska, M. J., Joseph, N. M. and Easter, S. S. (2000). Modulation of cell proliferation in the embryonic retina of zebrafish (Danio rerio). *Dev. Dyn.* **219**, 391-401.

Morais-de-Sa, E. and Sunkel, C. (2013). Adherens junctions determine the apical position of the midbody during follicular epithelial cell division. *EMBO Rep.* **14**, 696-703.

Parameswaran, S., Xia, X., Hegde, G. and Ahmad, I. (2014). Hmga2 regulates self-renewal of retinal progenitors. *Development* **141**, 4087-4097.

Poggi, L., Vitorino, M., Masai, I. and Harris, W. A. (2005). Influences on neural lineage and mode of division in the zebrafish retina in vivo. *J. Cell Biol.* **171**, 991-999.

Pollarolo, G., Schulz, J. G., Munck, S. and Dotti, C. G. (2011). Cytokinesis remnants define first neuronal asymmetry in vivo. *Nat. Neurosci.* **14**, 1525-1533.

Pujic, Z., Omori, Y., Tsujikawa, M., Thisse, B., Thisse, C. and Malicki, J. (2006). Reverse genetic analysis of neurogenesis in the zebrafish retina. *Dev. Biol.* **293**, 330-347.

Reyes, C. C., Jin, M., Breznau, E. B., Espino, R., Delgado-Gonzalo, R., Goryachev, A. B. and Miller, A. L. (2014). Anillin regulates cell-cell junction integrity by organizing junctional accumulation of rho-GTP and actomyosin. *Curr. Biol.* **24**, 1263-1270.

Riedl, J., Crevenna, A. H., Kessenbrock, K., Yu, J. H., Neukirchen, D., Bista, M., Bradke, F., Jenne, D., Holak, T. A., Werb, Z. et al. (2008). Lifeact: a versatile marker to visualize F-actin. *Nat. Methods* **5**, 605-607.

Rincon, S. A. and Paoletti, A. (2012). Mid1/anillin and the spatial regulation of cytokinesis in fission yeast. *Cytoskeleton (Hoboken)* **69**, 764-777.

Ronkainen, H., Hirvikoski, P., Kauppila, S. and Vaarala, M. H. (2011). Anillin expression is a marker of favourable prognosis in patients with renal cell carcinoma. *Oncol. Rep.* **25**, 129-133.

Schuhmacher, L.-N., Albadri, S., Ramialison, M. and Poggi, L. (2011). Evolutionary relationships and diversification of barhl genes within retinal cell lineages. *BMC Evol. Biol.* **11**, 340.

Shi, S.-H., Jan, L. Y. and Jan, Y.-N. (2003). Hippocampal neuronal polarity specified by spatially localized mPar3/mPar6 and PI 3-kinase activity. *Cell* **112**, 63-75.

Singh, D. and Pohl, C. (2014). Coupling of rotational cortical flow, asymmetric midbody positioning, and spindle rotation mediates dorsoventral axis formation in C. elegans. *Dev. Cell* **28**, 253-267.

Takekuni, K., Ikeda, W., Fujito, T., Morimoto, K., Takeuchi, M., Monden, M. and Takai, Y. (2003). Direct binding of cell polarity protein PAR-3 to cell-cell adhesion molecule nectin at neuroepithelial cells of developing mouse. *J. Biol. Chem.* **278**, 5497-5500.

Zolessi, F. R., Poggi, L., Wilkinson, C. J., Chien, C.-B. and Harris, W. A. (2006). Polarization and orientation of retinal ganglion cells in vivo. *Neural Dev.* **1**, 2.

DEVELOPMENT